

Supplementary Information
for
Effect of the Substitution Pattern (Peripheral vs Non-peripheral) on
the Spectroscopic, Electrochemical, and Magnetic Properties of
Octahexylsulfanyl Copper Phthalocyanines

Tulin Ateş Turkmen^a, Lihan Zeng^b, Yan Cui^b, İsmail Fidan,^c Fabienne Dumoulin^{c*}, Catherine Hirel^c, Yunus Zorlu^c, Vefa Ahsen^c, Alexander A. Chernonosov,^d Yurii Chumakov^{a,e}, Karl M. Kadish^{b*}, Ayşe Gül Gürek^{c*} and Sibel Tokdemir Öztürk^{a*}

^a *Gebze Technical University, Department of Physics, 41400 Gebze, Kocaeli, Turkey*

^b *Department of Chemistry, University of Houston, Houston, TX 77204-5003, USA*

^c *Gebze Technical University, Department of Chemistry, 41400 Gebze, Kocaeli, Turkey*

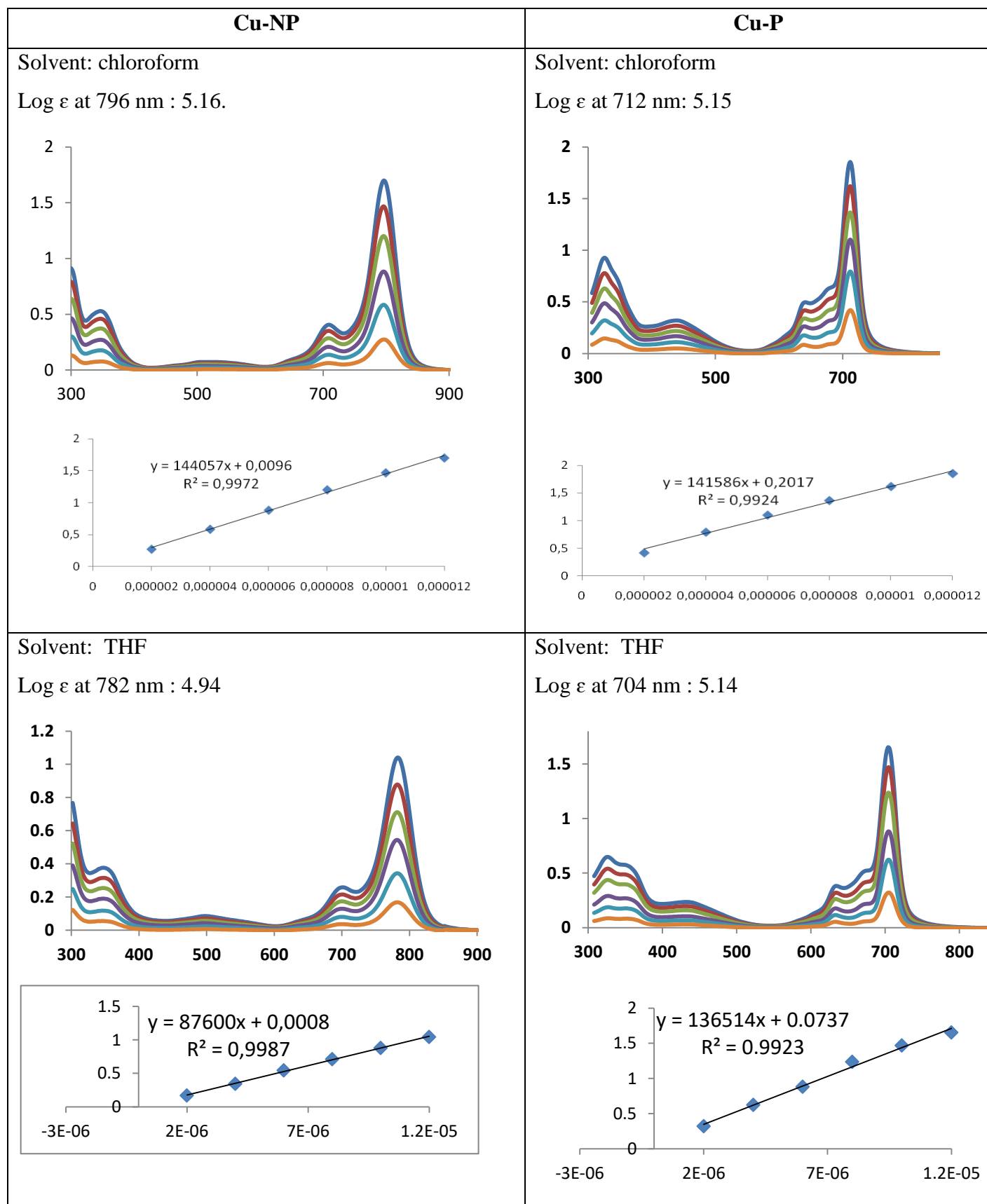
^d *Institute of Chemical Biology and Fundamental Medicine, 8 Lavrentiev Avenue, Novosibirsk 630090, Russia*

^e *Institute of Applied Physics of the Academy of Sciences of Moldova, Academiei str. 5, Chisinau, Moldavia*

Content

	Page
Table S1. UV-Vis spectra (2 to 12 μ M)	S3
Figure S1. Observed P-XRD profiles for Cu-P and Cu-NP .	S4
Figure S2. View of optimized geometry of Cu-P (top) and Cu-NP (bottom) in the gas phase	S5
Figure S3. 3D plots of the HOMO and LUMO for X-ray structure of Cu-NP .	S6
Figure S4. 3D plots of the HOMO and LUMO for model of Cu-P .	S7
Figure S5. 3D plots of the HOMO and LUMO for model of Cu-NP	S8
Figure S6. FT-IR spectra of Cu-P and Cu-NP	S9
Figure S7. MALDI-MS spectra of Cu-P and Cu-NP	S10
HRMS experimental details and mass accuracy	S11
Figure S8. MALDI-TOF HRMS spectrum of Cu-P	S12
Figure S9. MALDI-TOF HRMS spectrum of Cu-NP	S13
Experimental details and results of the elemental analyses	S14
Figure S10. Scan of the report of the elemental analysis results.	S14
Table S2. Crystal data and refinement parameters for Cu-NP	S15
Table S3. Selected bond lengths and angles for Cu-NP .	S16
Table S4. Angles between the normals of opposite isoindole units	S17
Figure S11. Crystal structures of non-peripherally octa hexylsulfanyl-substituted phthalocyanines Cu-NP , JUPBON, AJUVIK-01, AJUVIK-1A and AJUVIK-1B	S17
Figure S12. Total spin density plots for X-ray structure of Cu-NP and Cu-P .	S18

Table S1. UV-Vis spectra (2 to 12 μM)



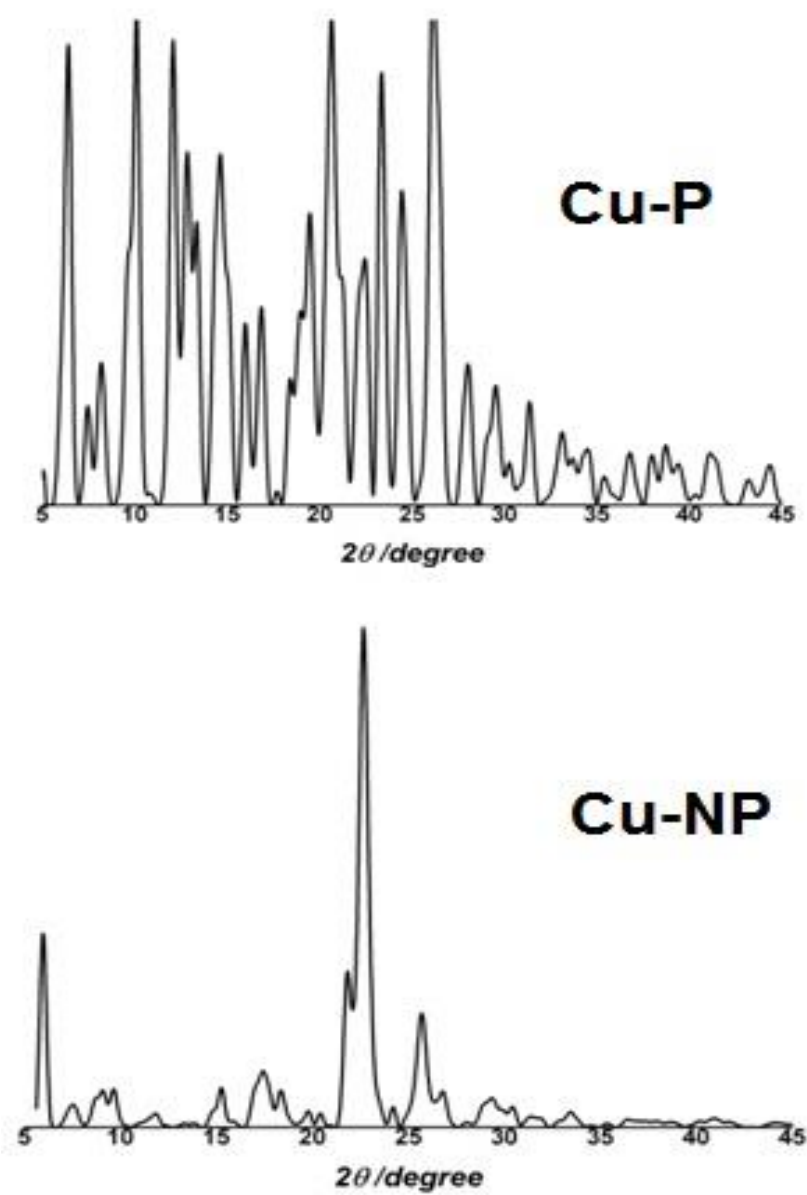


Figure S1. Observed P-XRD profiles for **Cu-P** and **Cu-NP**.

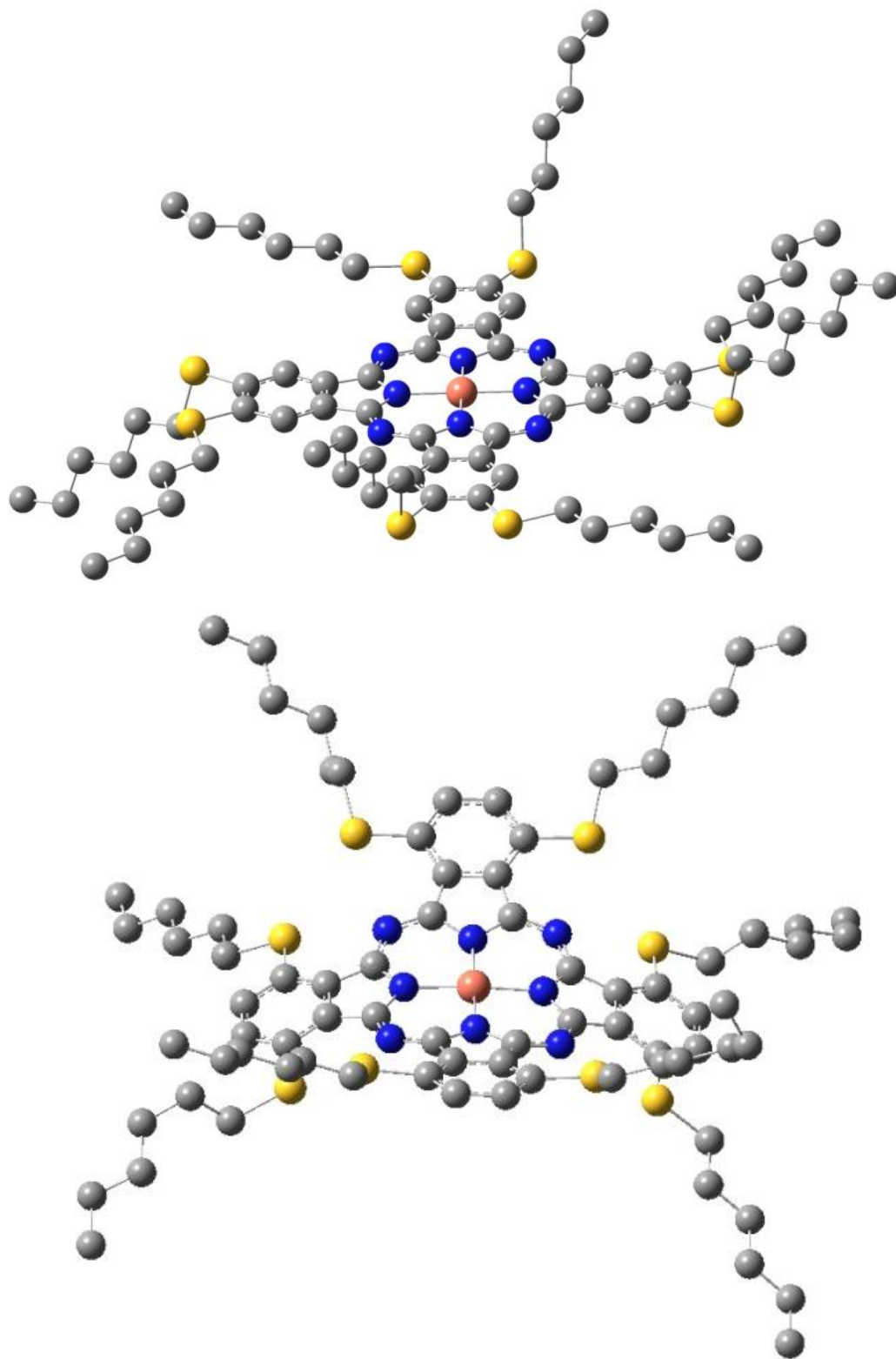


Figure S2. View of optimized geometry of **Cu-P** (top) and **Cu-NP** (bottom) in the gas phase. Atom colors: C (Grey), N (blue), Cu (orange), and S (yellow)

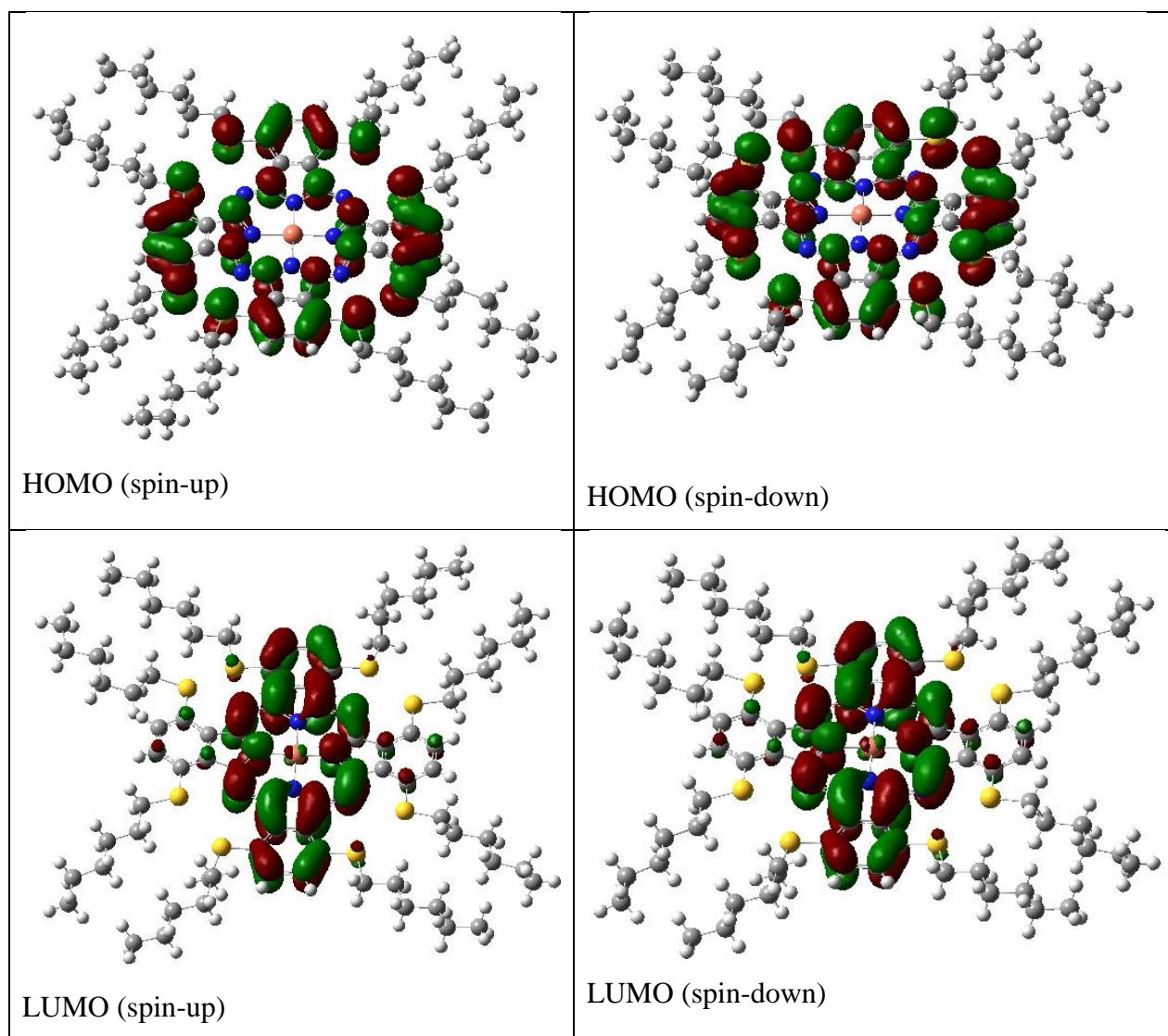


Figure S3. 3D plots of the HOMO and LUMO for X-ray structure of **Cu-NP**.

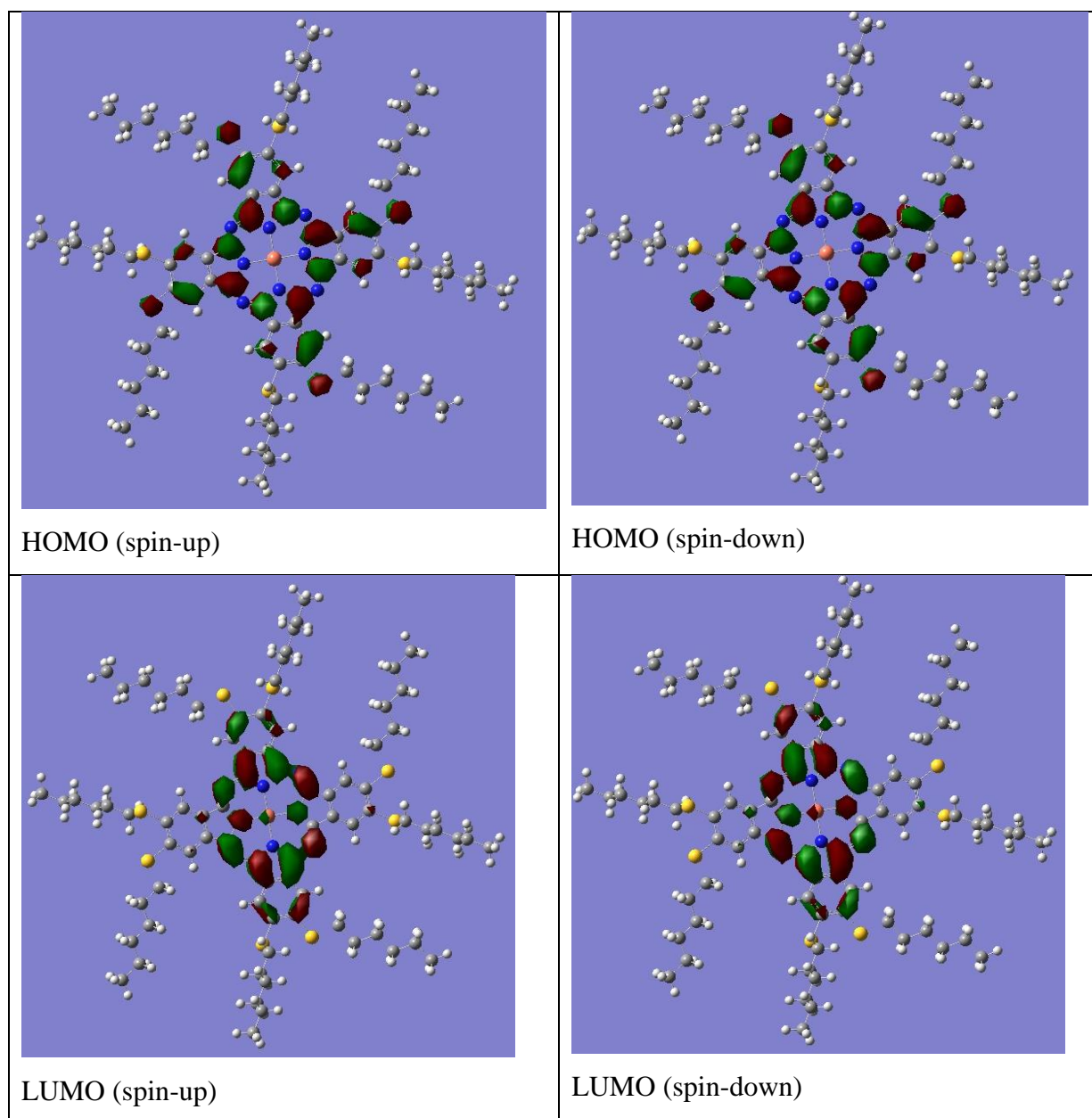


Figure S4. 3D plots of the HOMO and LUMO for model of **Cu-P**.

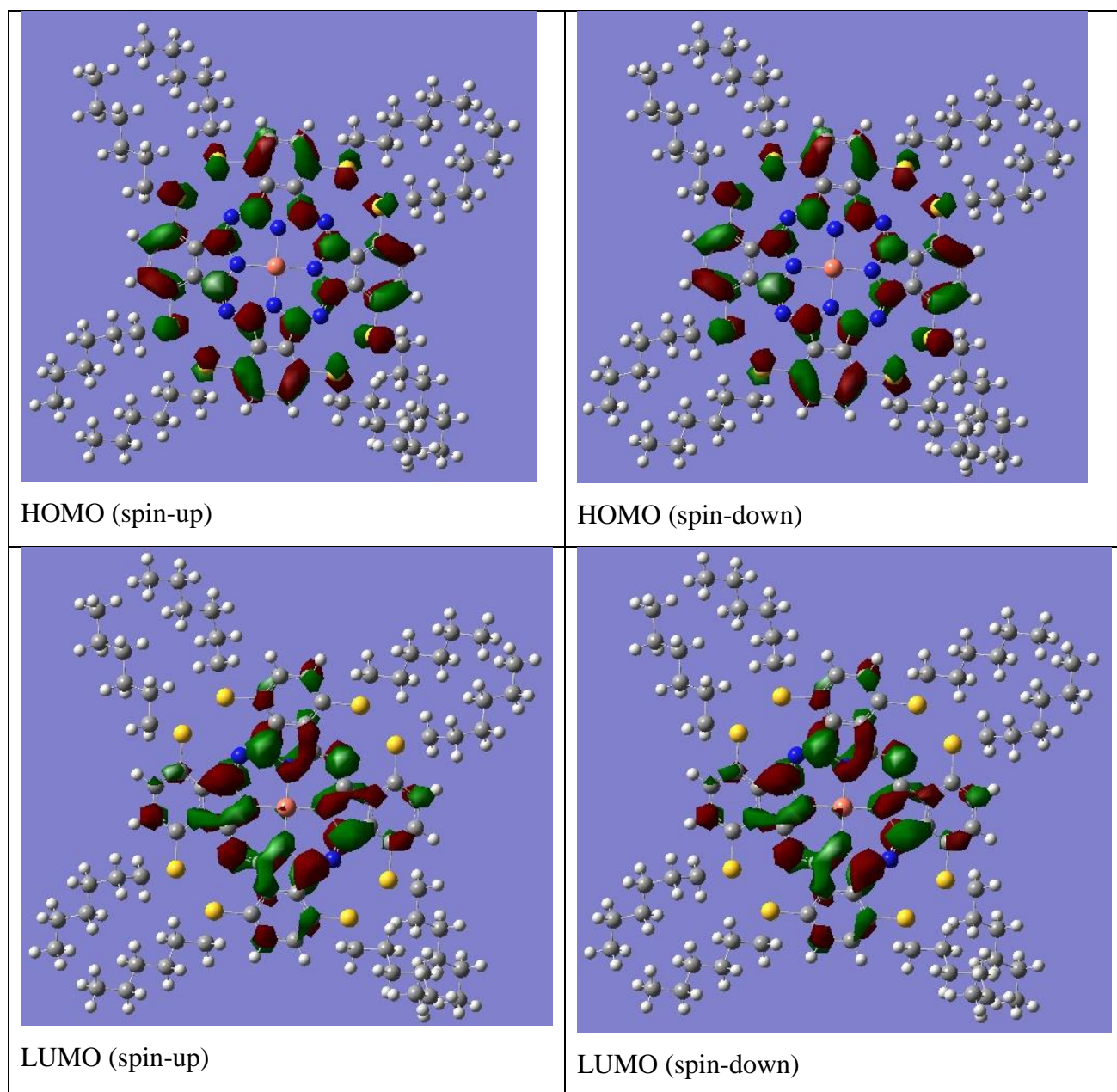


Figure S5. 3D plots of the HOMO and LUMO for model of **Cu-NP**.

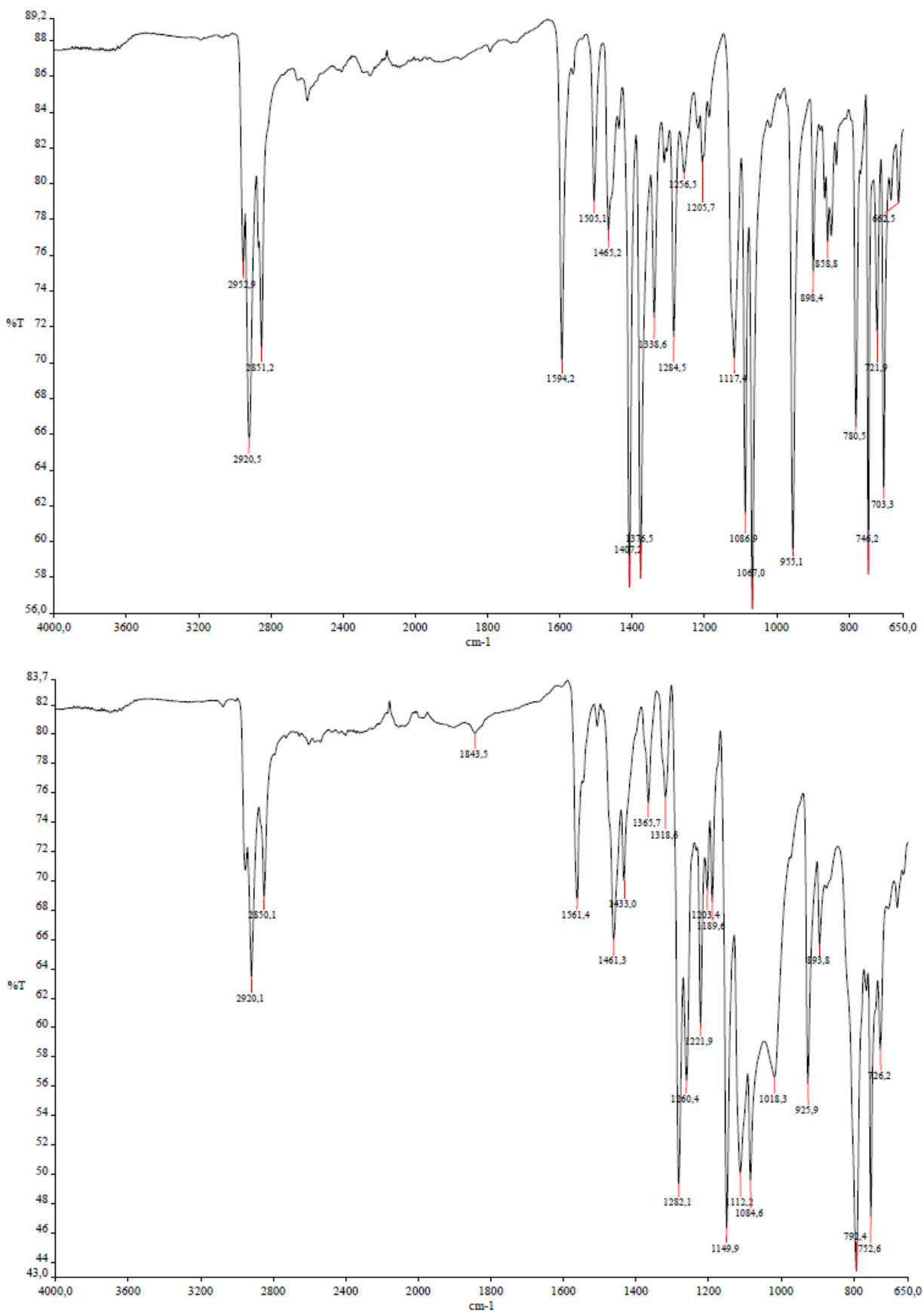


Figure S6. FT-IR spectra of **Cu-P** (top) and **Cu-NP** (bottom).

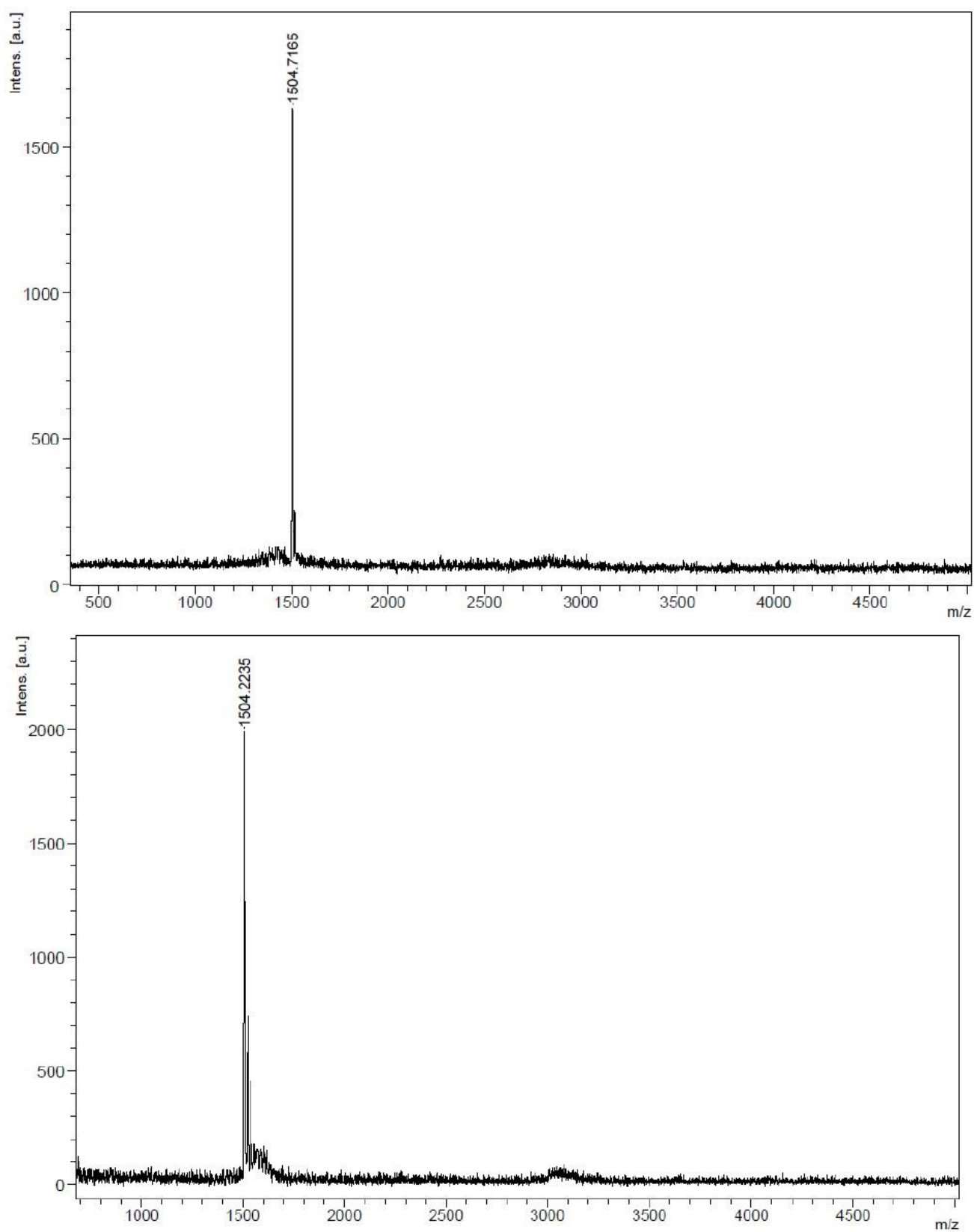


Figure S7. MALDI-MS spectra of **Cu-P** (top, matrix: 2,5-dihydroxybenzoic acid) and **Cu-NP** (bottom, matrix: dithranol).

HRMS experimental details and mass accuracy

High-resolution MALDI spectra for **Cu-NP** and **Cu-P** were obtained in matrix free conditions. Sample was dissolved in THF and one μL was spotted on the MTP 384 polished steel plate. Sample was allowed to air dry before the target was loaded into the mass spectrometer. Mass spectra were obtained in positive reflectron ion mode using Autoflex Speed MALDI-TOF mass spectrometer (Bruker Daltonics, Bremen, Germany) with an acceleration voltage of 19 kV (Ion source 1), 16.75 kV (Ion source 2), 8.75 kV (Lens), 21 kV (Reflector 1), 9.7 kV (Reflector 2) and laser frequency of 1 Hz. The reflector multiplayer was set at 16. The laser power was set at 40% to 100% of the maximum. Signals from 500 shots were accumulated for each spectrum. For external calibration the standard peptide mixture “Peptide Mix II” (Bruker Daltonics) was used.

HRMS (MALDI-TOF) m/z $[\text{M}]^+$ calculated for $\text{C}_{80}\text{H}_{112}\text{CuN}_8\text{S}_8$ 1505.6074; found 1505.6070 (mass accuracy 0.27 ppm) for **Cu-P** and found 1505.6073 (mass accuracy 0.07 ppm) for **Cu-NP**.

For **Cu-P**, the resolution of the spectrum is about 13500 FWHM.

The mass accuracy is 0.27 ppm: 1505.6074 (calculated) - 1505.6070 (found) = 0.0004 Da

$$0.0004/1505.6074 * 1000000 = 0.27 \text{ ppm}$$

For **Cu-NP**, the resolution of the spectrum is about 13500 FWHM

The mass accuracy is 0.07 ppm:

$$1505.6074 \text{ (calculated)} - 1505.6073 \text{ (found)} = 0.0001 \text{ Da}$$

$$0.0001/1505.6074 * 1000000 = 0.07 \text{ ppm}$$

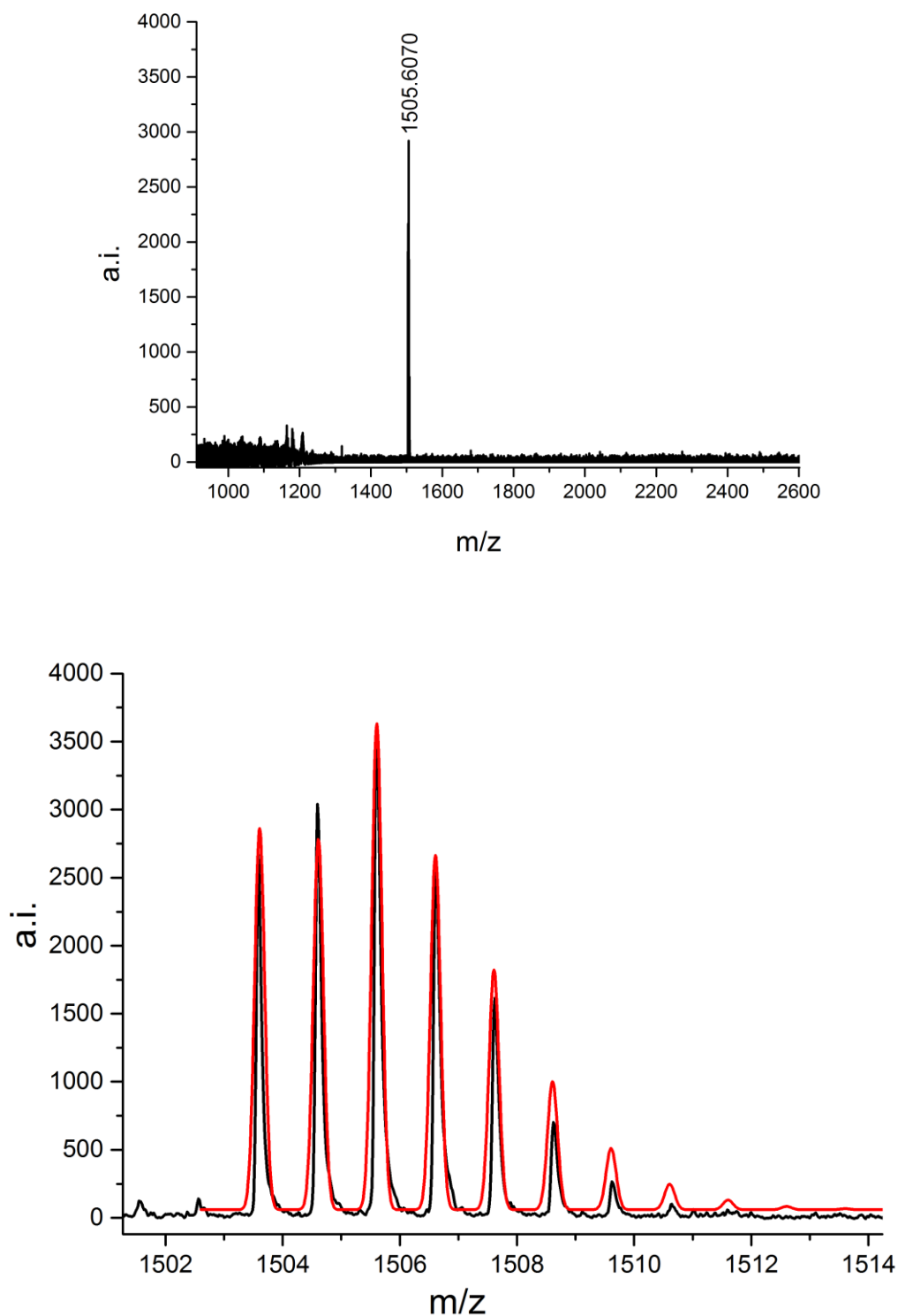


Figure S8. MALDI-TOF high-resolution mass spectrum of **Cu-P**. Top: full spectrum, bottom: superposition of the theoretical (red) and experimental (black) isotopic patterns. The observed molecular ion is $[M]^+$. Mass accuracy 0.27 ppm.

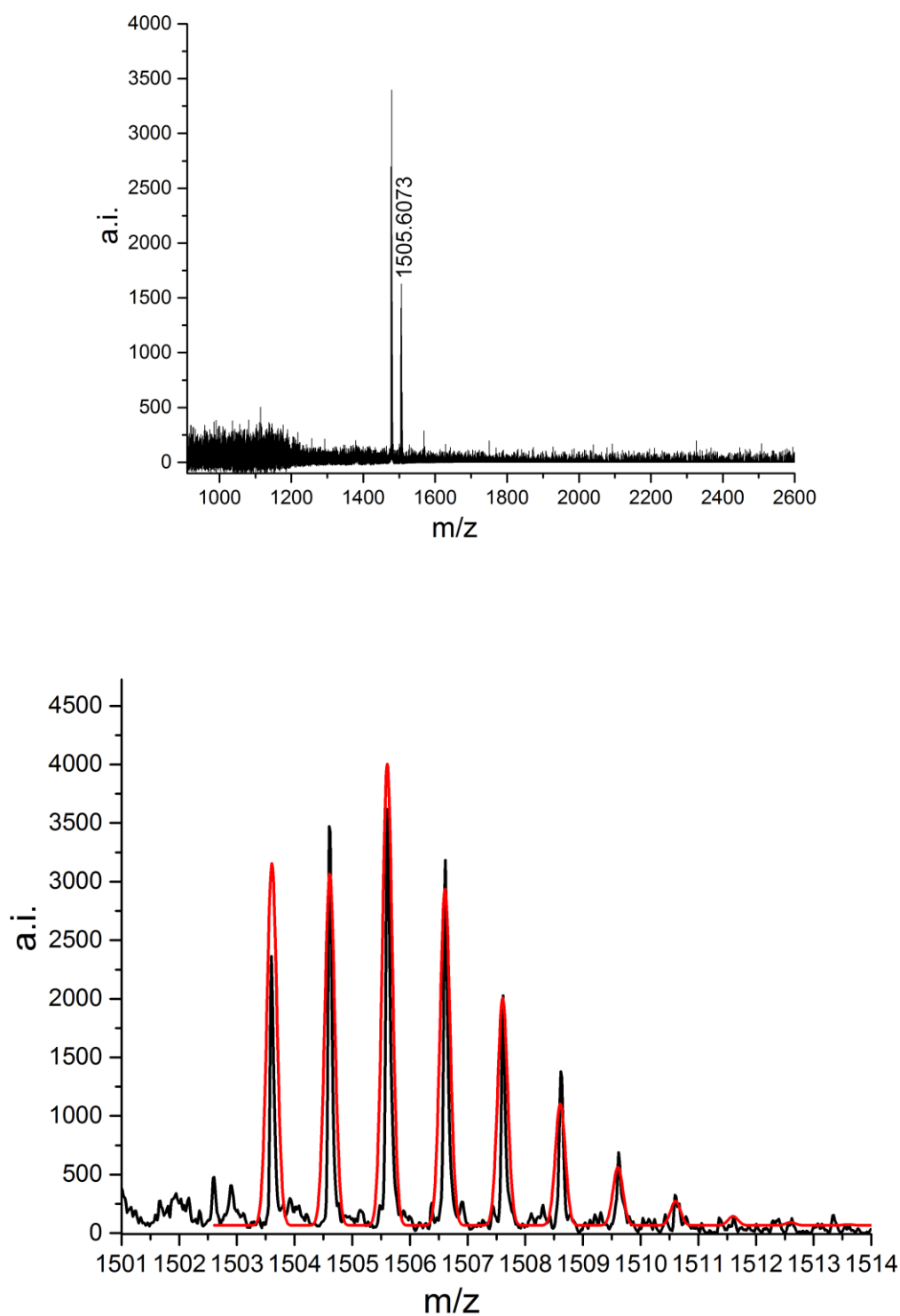


Figure S9. MALDI-TOF high-resolution mass spectrum of **Cu-NP**. Top: full spectrum, bottom: superposition of the theoretical (red) and experimental (black) isotopic patterns. The observed molecular ion is $[M]^+$. Mass accuracy 0.07 ppm.

Experimental details and results of the elemental analyses

Elemental analyses were carried out on an ECS 4010 Costech Instruments Elemental Combustion System (CHNS).

Elemental analysis calc. for $C_{80}H_{112}CuN_8S_8$ (MW 1505.858):

C, 63.81; H, 7.50; Cu, 4.22; N, 7.44; S, 17.03

Found for **Cu-P**: C, 63.77; H, 7.56; N, 7.19; S, 17.14.

Found for **Cu-NP**: C, 63.78; H, 7.51; N, 7.51; S, 17.04.

08.02.2018 15:32 Chromatogram C:\EAS Clarity\Giresun Merkez Lab.\Sonuç\np-sr-cupc_07_02_2018_21_33_85.PRM

Giresun Üniversitesi
Merkez Araştırma Laboratuvarı Uygulama ve Araştırma Merkezi

Method	: C:\EAS Clarity\Giresun Merkez Lab\NCHS	By	: TRL
Description	: NCHS		
Created	: 29.09.2006 12:30	Modified	: 08.02.2018 15:29
GC Column	: SS 6x5 mm - 2 m - HayeSep Q 60/80	Left Furnace Temp	: 1020°C
Detection	: TCD: L-3	Right Furnace Temp	: off
Flow Rate	: 100 ml/min	Oven Temperature	: 75°C
Note	: Reaction tube: 450x18 mm Packing: standard for NCHS O2 loop: 5 ml - 100 kPa		

Summary Table										
		Sample	Nitrogen		Carbon		Hydrogen		Sulphur	
			Response	Weight [%]	Response	Weight [%]	Response	Weight [%]	Response	Weight [%]
INT7 - 1	dnm1_07_02_2018_12_38_47	dnm1	134,369	6.54	3403,609	72.60	716,433	6.16	135,873	7.52
	np-sr-cupc tkr_07_02_2018_21_	np-sr-cupc tkr	119,999	7.51	2454,540	63.78	631,927	7.51	238,969	17.04
	psr-cupc_07_02_2018_21_58_8	psr-cupc	148,298	7.19	2964,081	63.77	940,533	7.56	411,954	17.14

Figure S10. Scan of the report of the elemental analysis results. Calculated values for the BBOT standard are C, 72.53; H, 6.09; N, 6.51; S, 7.44. Found (first row of the table): C, 72.60; H, 6.16; N, 6.54; S, 7.52.

Table S2. Crystal data and refinement parameters for **Cu-NP**.

CCDC number	1470853
Empirical formula	C ₈₀ H ₁₁₂ CuN ₈ S ₈
Formula weight (g.mol ⁻¹)	1505.79
Temperature (K)	173(2)
Wavelength (Å)	0.71073
Crystal system	Triclinic
Space group	<i>P</i> -1
<i>a</i> (Å)	12.4291(9)
<i>b</i> (Å)	17.3435(14)
<i>c</i> (Å)	19.8523(14)
α(°)	64.475(3)
β(°)	84.337(4)
γ(°)	84.143(4)
<i>V</i> (Å ³)	3834.5(5)
<i>Z</i>	2
ρ _{calcd} (g.cm ⁻³)	1.304
μ (mm ⁻¹)	0.552
<i>F</i> (000)	1610
Crystal size (mm)	0.128 x 0.273 x 0.508
θ range for data collection (°)	2.94 - 25.68
<i>h/k/l</i>	-14/15, -17/21, -22/24
Reflections collected	61277

Independent reflections	14515 [R(int) = 0.0634]
Coverage of independent reflections (%)	99.7
Refinement method	Full-matrix least-squares on F ²
Data / restraints / parameters	14515 / 76 / 882
Goodness-of-fit on F ²	1.045
Final <i>R</i> indices [I>2sigma(I)]	<i>R</i> ₁ = 0.0598, w <i>R</i> ₂ = 0.1454
<i>R</i> indices (all data)	<i>R</i> ₁ = 0.0818, w <i>R</i> ₂ = 0.1596
(Δρ) _{max} and (Δρ) _{min} (e.Å ⁻³)	1.601 and -1.209

Table S3. Selected bond lengths and angles for **Cu-NP**.

Bond Lengths (Å)			
Cu1-N1	1.967(2)	Cu1-N2	1.957(2)
Cu1-N3	1.953(2)	Cu1-N4	1.959(2)
C2-N7	1.336(4)	C3-N7	1.327(4)
Bond Angles (Å)			
N3-Cu1-N2	90.08(10)	N3-Cu1-N4	90.29(10)
N2-Cu1-N4	178.71(11)	N3-Cu1-N1	177.11(10)
N2-Cu1-N1	89.64(10)	N4-Cu1-N1	90.05(10)
C1-N1-Cu1	125.5(2)	C3-N2-Cu1	126.1(2)
N7-C2-N1	127.1(3)	N7-C3-N2	127.6(3)

Table S4. Angles between the normals of opposite isoindole units.

Compound (CSD Ref. Code)	Angle between green isoindole units	Angle between red isoindole units	Reference
Cu-NP	12.18°	11.58°	this work
JUBPON	6.07°	15.19°	Zorlu, Y.; Kumru, U.; Isci, U.; Divrik, B.; Jeanneau, E.; Albrieux, F.; Dede, Y.; Ahsen, V.; Dumoulin, F. <i>Chem. Commun.</i> , 2015 , 5, 6580-6583
AJUVIK01	14.19°	24.71°	Burnham, M.; Chambrier, M. I.; Hughes, D. L.; Isare, B.; Poynter, R. J.; Powell, A. K.; Cook, M. J. <i>J. Porphyrins Phthalocyanines</i> . 2006 , 10, 1202-1211
AJUVIK-1A*	15.51°	22.49°	Burnham, P. M.; Cook, M. J.; Gerrard, L. A.; Heeney, M. J.; Hughes, D. L. <i>Chem. Commun.</i> 2003 , 16, 2064-2065
AJUVIK-1B*	11.20°	15.14°	Burnham, P. M.; Cook, M. J.; Gerrard, L. A.; Heeney, M. J.; Hughes, D. L. <i>Chem. Commun.</i> 2003 , 16, 2064-2065

*represents the crystallographically independent molecule in the asymmetric unit.

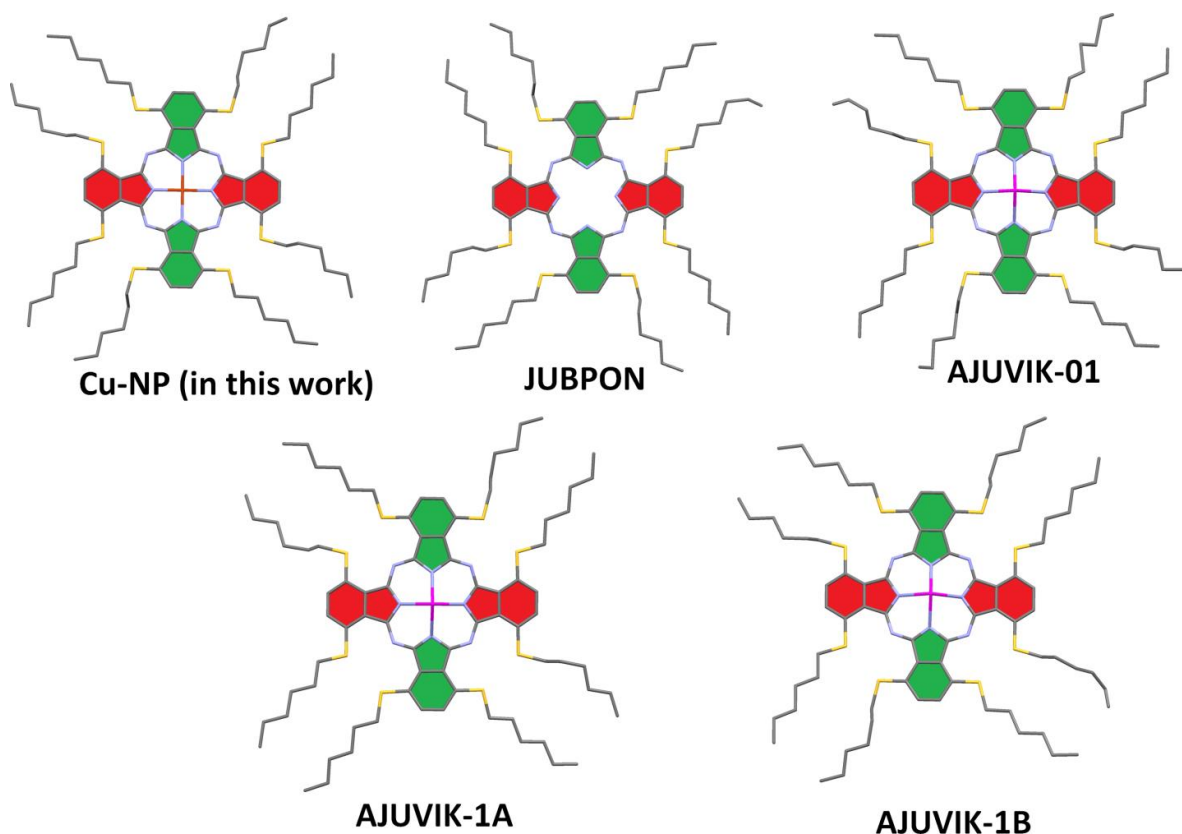
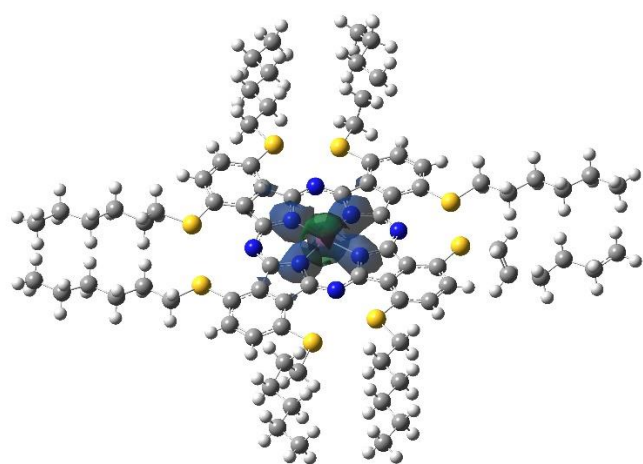
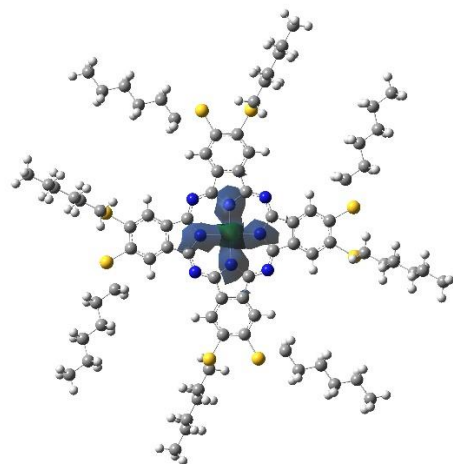


Figure S11. Crystal structures of non-peripherally octa hexylsulfanyl-substituted phthalocyanines **Cu-NP**, **JUBPON**, **AJUVIK-01**, **AJUVIK-1A** and **AJUVIK-1B** (see Table S4 for related references). The opposite isoindole units are shown in green and red colors. **AJUVIK-1A** and **AJUVIK-1B** are the crystallographically independent molecules in the asymmetric unit.



Cu-NP



Cu-P

Figure S12. Total spin density plots for X-ray structure of **Cu-NP** and **Cu-P**.